解産物（FDP)]，糖尿病関連検査［血中グルコース，グリコヘモグロビン（Hb_{A1C}）は血液検体で測定］をそれぞれ実施した．これら全ての検査を株式会社エスアールエル（東京）に依頼した．比較はHb小胞体添加血液に生理食塩水を添加し得られた血清または血漿と，生理食塩水添加血液にDexまたは生理食塩水を添加し得られた血清または血漿とした．また血清採取用真空採血管は凝固促進剤，血清分離剤が収容されているものなど幾つか種類があるので（Fig. 3の採血管収容物を参照），採血管の違いによる影響も調べた．干渉作用の有無の判定では，米国FDAのClinical Laboratory Improvement Amendments（CLIA）の規定する臨床試験に関する測定誤差の許容範囲（CLIA limit）を判断基準とし[5,6]，基準値との較差（誤差）が許容範囲を正に超える項目を（↑），負較差を与える項目を（↓）と表記した．また，基準値との較差が許容範囲である場合には干渉作用無（none）と判断した．CLIA limitが規定されていない項目に関しては，較差の許容範囲を20％として判定した．今回はコントロールとの比較による干渉の有無の判定を目的としたため，血液にHb小胞体，Dex溶液ないし生理食塩水を添加して希釈率を統一（1.35倍希釈）して比較した．希釈率の補正は行っていない．

3．結果および考察

3.1．Dex添加によるHb小胞体の凝集

まず，Hb小胞体に各種分子量のDexを添加し，溶液濁度変化（Δ O.D.）を経時的にモニターした結果をFig. 1に示す．分子量72.1 kDa以下のDexをHb小胞体に添加してもほとんど溶液濁の変化を認めないが，分子量124 kDaのDexでは溶液濁度の上昇が観測され，さらに分子量487 kDaのDex添加により著しい溶液濁度の増大が観測された．粒子による光散乱強度は粒子径の6乗に比例するため，凝集による粒子径の増大は溶液濁度の増大（光散乱強度の増大）として検出される．高分子添加により懸濁粒子が凝集する現象はよく知られ，リン脂質小胞体は共存する高分子との相互作用が比較的詳しく調べられている[21-24]．高分子による小胞体凝集の主要な作用として，小胞体表面の電荷（ゼータ電位）の中和あるいは遮蔽による粒子の不安定化，小胞体間の架橋，高分子による粒子の排除（枯乾効果）などが知られ，一般に同一の繰り返し単位を有する高分子であれば高分子量体ほど凝集能が高く，凝集生起の臨界分子量の存在が認められる[23]．今回の結果より，分子量487 kDa程度のDexがHb小胞体の凝集に適していると考えられる．Hb小胞体の凝集は数分間で進行するため，Dexを添加してHb小胞体を凝集させる条件を室温（25℃）で10分間静置に設定した．

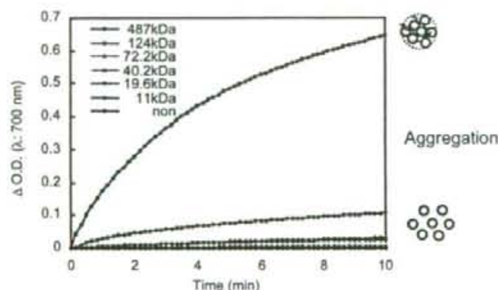

Fig. 1. Kinetics of aggregation of HbV in the presence of 1.8％ dextran at 25℃. Dex solution was added to the HbV dispersion. Increase of the ΔO.D. indicates the formation of larger aggregate of HbV by the addition of Dex.

3.2．血清分離条件の検討

Hb小胞体の浮遊する採血液に対し分子量の異なるDex溶液を添加し，10分間静置した後に遠心分離した採血管をFig. 2aに示す（Dex終濃度：1.8 g/dl）．Dex分子量の効果は明確で，487 kDaのDexを添加した系のみ透明な血漿が得られた．124 kDaではHb小胞体の沈殿を認めるものの不十分であり，それ以下の分子量では沈殿を認めなかった．遠心加速度（$r\omega^2$）による粒子の沈降速度（v）は次の式（1）で表すことができる．

$$v = \frac{d^2}{1.8} \times \frac{(\sigma\ \rho)}{\eta} \times r\omega^2 \qquad (1)$$

ここで，d (cm)：粒子の直径，σ (g/cm^3)：粒子の密度，ρ (g/cm^3)：溶液の密度，η (g・cm^{-1}・s^{-1})：溶液の粘度．
沈降速度は粒子直径の2乗に比例するため，凝集により見かけ上の粒子の直径を大きくすることで沈降速度が増大する．Fig. 1の結果との対応から，Dex 487 kDa の添加によるHb小胞体の著しい凝集により遠心で沈降できる大凝集体が生起するものと考えられる．この結果より，Dexの分子量を487 kDaに設定した．

次に，Dex 487 kDaの濃度条件を検討した．7 ml採血管（プレーン）に高分子凝集剤としてDex 487kDaの0.3～0.75 mLを添加した採血管を作成し，採血液（5 ml）を各採血管に採取して，25℃で10分間静置した．この混合液を遠心分離（5000 rpm，10分）して血漿層からのHb小胞体の除去の有無を観測した．結果として，透明な血漿層が得られるのはDex 487kDaを終濃度で1.8 g/dl以上添加した場合であり，更に血漿層を超遠心分離して分析すると，2.6 g/dl以上でほぼ完全にHb小胞体が除去されることを確認した（Fig. 2b）．血漿層にHb由来の吸収はなくDex 487kDa添加による赤血球やHb小胞体の溶血もない．沈殿物は下層の血球層と上層のHb小胞体で明らかな界面を認め，容易に各々の沈降占有容積率（クリット値）を計測できる．またHb小胞体の沈殿と血漿の界面も明確であるため，血漿採取は比較的容易である．以上より，Hb小胞体投与後には，Dex 487kDaが終濃度2.6 g/dlとなるように封入された採血管を使用すれば，従来通りの遠心分離にて濁度やHb吸収の干渉作用のない血漿ないし血清を採取できることが示された．

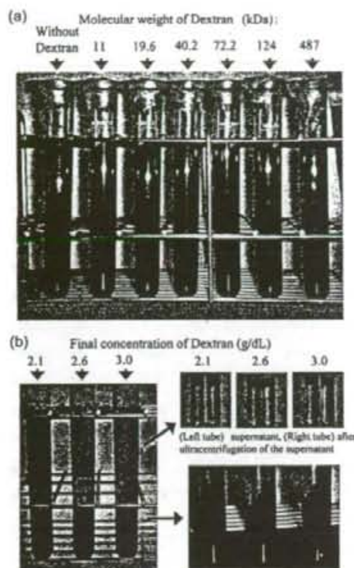

Fig. 2. Precipitation of the aggregated HbV by centrifugation. (a) Effect of the molecular weight of the Dex. (b) Effect of the concentration of the Dextran. HbV could be precipitated in centrifugation of blood sample in presence of 2.6 g/dL Dex (Mw. 487 kDa). Aggregated HbV forms pellet on a red blood cell pellet after centrifugation.

3.3. ヒト血液検体検査

高分子量Dex添加によりHb小胞体を除去する方法について，血液検体検査への適合性をヒト血清，血漿の外観と検査結果で評価した．Hb小胞体添加血液に生理食塩水を加えて遠心分離した血清，血漿はHb小胞体が浮遊しているため赤色であった．しかしDex添加によりHb小胞体を除去した血清と血漿（Fig. 3）は一部の血清採取用採血管（Fig. 3c, d）で少し赤みが帯びていたもののほぼ黄色であった．赤みが帯びていた血清はDexと血液の混和が不十分であったためHb小胞体を除去しきれなかったことが考えられる．Hb小胞体の除去効果は血清，血漿の外観から肉眼で確認可能であった．各検査においてHb小胞体浮遊血清，血漿は以下のような干渉作用を示した．生化学検査（Table 1～3）においては総タンパク，アルブミン，LDH，CK，クレアチニン，CRP，ハプトグロビンの上昇が見られた．また，総コレステロール，エステル型コレステロール，遊離型コレステロール，リン脂質ではHb小胞体の脂質膜が影響し上昇した．尿素窒素とIgMは低下し，ChEは低下傾向を示した．総ビリルビン，AST，ALT，γGTPにおいては検査不能と判断された．免疫学検査項目であるHBs抗原・抗体，HCV抗体いずれもHb小胞体による影響は認められなかった．これらの結果は4種すべての血清採取用採血管で同様であった．生化学・免疫学検査の全32項目中，Hb小胞体の干渉作用により適切な測定値が得られない項目は17ないし18項目に上った（Table 1～3）．一方，Dexの添加によりHb小胞体を除去することで，3ないし4項目（遊離脂肪酸，リポプロテイン，遊離コレステロール，フェリチン，ALT，AST）を除き適切

採血管収容物	検査項目
(a) プレイン（収容物なし）	＜生化学・免疫学検査＞ 総タンパク，アルブミン，総ビリルビン，AST，ALT，g-GTP，LDH，LAP，CK，ChE，尿素窒素，尿酸，総コレステロール，エステル型コレステロール，遊離型コレステロール，トロンボポエチン(A)，トリグリセライド，リン脂質，遊離脂肪酸，HDL-C定量，カリウム，カルシウム，無機リン，クレアチニン，CRP定量，フェリチン，ハプトグロビン，IgG，IgM，HBs抗原，HBs抗体，HCV抗体
(b) 凝固促進フィルム	
(c) 血清分離剤 凝固促進フィルム	
(d) 血清分離剤 凝固促進フィルム トロンビン	
(e) 3.8% クエン酸ナトリウム	＜凝固線溶系検査＞ APTT，PT，ATIII，トータル PAI-1，フィブリノゲン，vWF抗原，vWF活性
(f) トロンビン アプロチニン 蛇毒	＜凝固線溶系検査＞ D-ダイマー，FDP
(g) フッ化ナトリウム	＜糖尿病関連検査＞ 血中グルコース

Fig. 3. Blood collecting tubes and analytes of clinical laboratory tests. (a)-(g) Blood samples after centrifugation. The blood collecting tube contain blood+saline+saline (control), blood+saline+Dex (interference effect of Dex), blood+HbV+saline (interference effect of HbV), or blood+HbV+Dex (this method).

Table 1. Clinical chemistry and immunological tests (Blood collection tube without contents)

Analytes	Units	CLIA limits	Blood+Saline			Blood+HbV			
			+Saline (Control)	+Dex	IF*	+Saline	IF*	+Dex	IF*
Total protein	g/dL	± 10%	5.1	4.8	none	14	↑	4.8	none
Albumin	g/dL	± 10%	3.3	3.2	none	4.3	↑	3.2	none
Total bilirubin	mg/dL	±0.4mg/dL or ± 20%	0.2	0.1	none	impossible	×	0.1	none
AST	IU/L	± 20%	11	10	none	impossible	×	10	none
ALT	IU/L	± 20%	7	7	none	impossible	×	7	none
γ-GTP	IU/L	± 20%	8	8	none	impossible	×	7	none
LDH	IU/L	± 20%	134	118	none	270	↑	127	none
LAP	IU/L	ND, ± 20%	63	62	none	58	none	64	none
CK	IU/L	± 30%	46	46	none	89	↑	47	none
ChE	IU/L	ND, ± 20%	243	242	none	215	none	247	none
Urea nitrogen	mg/dL	± 2 mg/dL or ± 9%	6.1	6.0	none	1.2	↓	6.3	none
Creatinine	mg/dL	±0.3 mg/dL or ± 15%	0.39	0.43	none	2.03	↑	0.47	none
Uric acid	mg/dL	± 17%	2.6	2.5	none	2.5	none	2.7	none
Total cholesterol	mg/dL	± 10%	129	119	none	334	↑	113	none
Cholesterol ester	mg/dL	ND, ± 20%	99	92	none	238	↑	92	none
Free cholesterol	mg/dL	ND, ± 20%	30	27	none	96	↑	21	↓
Triglyceride	mg/dL	± 25%	90	73	none	86	none	69	none
phospholipid	mg/dL	ND, ± 20%	163	156	none	235	↑	153	none
Free fatty acid	mEQ/L	ND, ± 20%	0.08	0.08	none	0.09	none	0.14	↑
HDL-C	mg/dL	ND, ± 20%	43	43	none	39	none	45	none
Lipoproteins	mg/dL	± 30%	12	5	↓	15	none	6	↓
K^+	mEQ/L	±0.5 mmol/L	2.4	2.5	none	2.5	none	2.6	none
Ca^{2+}	mg/dL	±0.25 mmol/L	6.2	6.2	none	5.9	none	6.2	none
Inorganic phosphate	mg/dL	ND, ± 20%	2.1	2.0	none	2.2	none	2.2	none
CRP	mg/dL	ND, ± 20%	≤ 0.02	≤ 0.02	none	0.1	↑	≤ 0.02	none
Ferritin	ng/mL	ND, ± 20%	3.5	3.0	none	3.4	none	2.8	↓
Haptoglobin	mg/dL	ND, ± 20%	80	74	none	117	↑	80	none
IgG	mg/dL	± 25%	747	734	none	655	none	744	none
IgM	mg/dL	ND, ± 20%	93	86	none	60	↓	88	none
HBs antigen	IU/mL	positive or negative	< 0.05	< 0.05	none	<0.05	none	< 0.05	none
HBs antibody	mIU/mL	positive or negative	< 10.0	< 10.0	none	< 10.0	none	< 10.0	none
HCV antibody		positive or negative	0.0	0.0	none	0.0	none	0.0	none

AST: aspartate aminotransferase, ALT: alanine aminotransferase, γ-GTP: γ-glutamyltranspeptitase, LDH: lactate dehydrogenase, LAP: leucine aminopeptidase, CK: creatine kinase, ChE: cholinesterase, HDL-C: high density lipoprotein cholesterol, CRP: C-reactive protein, HBs: hepatitis B surface, HCV: hepatitis C virus. * IF means interference. (↑)overestimation, (↓)underestimation, (none) no interference.

Table 2. Clinical chemistry and immunological tests (Blood collection tube containing clot activator)

Analytes	Units	CLIA limits	Blood+Saline			Blood+HbV			
			+Saline (Control)	+Dex	IF*	+Saline	IF*	+Dex	IF*
Total protein	g/dL	± 10%	5.2	4.8	none	14.3	↑	4.9	none
Albumin	g/dL	± 10%	3.3	3.2	none	4.2	↑	3.2	none
Total bilirubin	mg/dL	±0.4mg/dL or ± 20%	0.1	0.1	none	Impossible	×	0.1	none
AST	IU/L	± 20%	11	11	none	Impossible	×	12	none
ALT	IU/L	± 20%	5	8	↑	Impossible	×	8	↑
γ-GTP	IU/L	± 20%	7	7	none	Impossible	×	7	none
LDH	IU/L	± 20%	131	114	none	265	↑	115	none
LAP	IU/L	ND, ± 20%	61	62	none	58	none	62	none
CK	IU/L	± 30%	48	47	none	73	↑	48	none
ChE	IU/L	ND, ± 20%	239	236	none	220	none	241	none
Urea nitrogen	mg/dL	± 2 mg/dL or ± 9%	6.1	6.3	none	Impossible	×	5.9	none
Creatinine	mg/dL	±0.3 mg/dL or ± 15%	0.45	0.41	none	1.80	↑	0.42	none
Uric acid	mg/dL	± 17%	2.5	2.5	none	2.3	none	2.7	none
Total cholesterol	mg/dL	± 10%	126	126	none	333	↑	119	none
Cholesterol ester	mg/dL	ND, ± 20%	95	96	none	239	↑	91	none
Free cholesterol	mg/dL	ND, ± 20%	31	30	none	94	↑	28	none
Triglyceride	mg/dL	± 25%	88	80	none	82	none	69	none
phospholipid	mg/dL	ND, ± 20%	162	157	none	229	↑	157	none
Free fatty acid	mEQ/L	ND, ± 20%	0.08	0.08	none	0.09	none	0.15	↑
HDL-C	mg/dL	ND, ± 20%	41	42	none	39	none	43	none
Lipoproteins	mg/dL	± 30%	14	11	none	14	none	4	↓
K^+	mEQ/L	±0.5 mmol/L	2.4	2.4	none	2.5	none	2.6	none
Ca^{2+}	mg/dL	±0.25 mmol/L	6.0	6.1	none	5.7	none	6.0	none
Inorganic phosphate	mg/dL	ND, ± 20%	2.1	2.0	none	2.8	none	2.1	none
CRP	mg/dL	ND, ± 20%	≤ 0.02	≤ 0.02	none	0.08	↑	≤ 0.02	none
Ferritin	ng/mL	ND, ± 20%	2.8	2.5	none	2.8	none	2.6	none
Haptoglobin	mg/dL	ND, ± 20%	78	78	none	118	↑	82	none
IgG	mg/dL	± 25%	736	721	none	640	none	742	none
IgM	mg/dL	ND, ± 20%	90	84	none	55	↓	85	none
HBs antigen	IU/mL	positive or negative	< 0.05	< 0.05	none	< 0.05	none	< 0.05	none
HBs antibody	mIU/mL	positive or negative	< 10.0	< 10.0	none	< 10.0	none	< 10.0	none
HCV antibody		positive or negative	0.0	0.0	none	0.0	none	0.0	none

AST: aspartate aminotransferase, ALT: alanine aminotransferase, γ-GTP: γ-glutamyltranspeptitase, LDH: lactate dehydrogenase, LAP: leucine aminopeptidase, CK: creatine kinase, ChE: cholinesterase, HDL-C: high density lipoprotein cholesterol, CRP: C-reactive protein, HBs: hepatitis B surface, HCV: hepatitis C virus. * IF means interference. (↑)overestimation, (↓)underestimation, (none) no interference.

Table 3. Clinical chemistry and immunological tests (Blood collection tube containing clot activator, inert barrier material, and thrombin)

Analytes	Units	CLIA limits	Blood+Saline			Blood+HbV			
			+Saline (Control)	+Dex	IF*	+Saline	IF*	+Dex	IF*
Total protein	g/dL	± 10%	5.0	4.8	none	14.0	↑	5.0	none
Albumin	g/dL	± 10%	3.3	3.2	none	4.3	↑	3.2	none
Total bilirubin	mg/dL	±0.4mg/dL or ± 20%	0.1	0.1	none	Impossible	×	0.1	none
AST	IU/L	± 20%	9	11	↑	Impossible	×	11	↑
ALT	IU/L	± 20%	6	8	↑	Impossible	×	7	none
γ-GTP	IU/L	± 20%	8	7	none	Impossible	×	7	none
LDH	IU/L	± 20%	113	110	none	260	↑	117	none
LAP	IU/L	ND, ± 20%	61	62	none	59	none	63	none
CK	IU/L	± 30%	48	47	none	55	none	49	none
ChE	IU/L	ND, ± 20%	239	240	none	225	none	244	none
Urea nitrogen	mg/dL	± 2 mg/dL or ± 9%	5.9	6.1	none	0.2	↓	5.8	none
Creatinine	mg/dL	±0.3 mg/dL or ± 15%	0.39	0.40	none	1.90	↑	0.5	none
Uric acid	mg/dL	± 17%	2.6	2.6	none	2.6	none	2.7	none
Total cholesterol	mg/dL	± 10%	127	123	none	337	↑	121	none
Cholesterol ester	mg/dL	ND, ± 20%	95	93	none	245	↑	92	none
Free cholesterol	mg/dL	ND, ± 20%	32	30	none	92	↑	29	none
Triglyceride	mg/dL	± 25%	89	79	none	84	none	70	none
phospholipid	mg/dL	ND, ± 20%	161	160	none	232	↑	157	none
Free fatty acid	mEQ/L	ND, ± 20%	0.07	0.08	none	0.09	↑	0.14	↑
HDL-C	mg/dL	ND, ± 20%	40	41	none	40	none	43	none
Lipoproteins	mg/dL	± 30%	14	9	↓	13	none	4	↓
K^+	mEQ/L	±0.5 mmol/L	2.4	2.4	none	2.5	none	2.7	none
Ca^{2+}	mg/dL	±0.25 mmol/L	6.1	6.1	none	6.0	none	6.1	none
Inorganic phosphate	mg/dL	ND, ± 20%	1.9	1.9	none	2.3	↑	2.2	none
CRP	mg/dL	ND, ± 20%	≤ 0.02	≤ 0.02	none	0.08	↑	≤ 0.02	none
Ferritin	ng/mL	ND, ± 20%	3.1	2.6	none	2.7	none	2.6	none
Haptoglobin	mg/dL	ND, ± 20%	77	82	none	121	↑	83	none
IgG	mg/dL	± 25%	736	729	none	670	none	748	none
IgM	mg/dL	ND, ± 20%	89	85	none	60	↓	87	none
HBs antigen	IU/mL	positive or negative	< 0.05	< 0.05	none	< 0.05	none	< 0.05	none
HBs antibody	mIU/mL	positive or negative	< 10.0	< 10.0	none	< 10.0	none	< 10.0	none
HCV antibody		positive or negative	0.0	0.0	none	0.0	none	0.0	none

AST: aspartate aminotransferase, ALT: alanine aminotransferase, γ-GTP: γ-glutamyltranspeptitase, LDH: lactate dehydrogenase, LAP: leucine aminopeptidase, CK: creatine kinase, ChE: cholinesterase, HDL-C: high density lipoprotein cholesterol, CRP: C-reactive protein, HBs: hepatitis B surface, HCV: hepatitis C virus. * IF means interference. (↑)overestimation, (↓)underestimation, (none) no interference.

Table 4. Coagulation fibrinolysis examination

Analytes	Units	CLIA limits	Blood+Saline			Blood+HbV			
			+Saline (Control)	+Dex	IF*	+Saline	IF*	+Dex	IF*
APTT	second	±15%	38.5	41.2	none	Impossible	×	40.8	none
PT	second	± 15%	12.2	12.2	none	Impossible	×	11.9	none
fibrinogen	mg/dL	± 20%	157	149	none	Impossible	×	161	none
ATIII	%	ND, ± 20%	69	67	none	82	↑	70	none
vWF antigen	%	ND, ± 20%	48	34	↓	Impossible	×	43	none
vWF activity	%	ND, ± 20%	52	24	↓	Impossible	×	21	↓
Total PAI-1	ng/mL	ND, ± 20%	6	15	↑	3	↓	12	↑
FDP	μg/mL	ND, ± 20%	≤2	≤2	none	≤2	none	≤2	none
D-dimer	μg/mL	ND, ± 20%	0.22	0.2	none	≤0.10	↓	0.18	none

APTT: Activated partial thromboplastin time, PT: Prothrombin time, ATIII: Antithrombin Ⅲ, PAI-1: plasminogen activator inhibitor-1, FDP: fibrinogen degradation products. * IF means interference. (↑)overestimation, (↓)underestimation, (none) no interference.

Table 5. Blood sugar tests

Analytes	Units	Blood+Saline			Blood+HbV			
		+Saline (Control)	+Dex	IF*	+Saline	IF*	+Dex	IF*
Glucose	mg/dL	65	66	none	57	none	69	none

Analytes	Units	Blood+Saline	Blood+HbV	IF
Hb_{A1C}	%	4.8	4.8	none

Hb_{A1C}: glycated hemoglobin. * IF means interference. (↑)overestimation, (↓)underestimation, (none) no interference.

な測定値が得られた．遊離コレステロール，フェリチン，ALT，ASTの干渉作用は試験管によるため，検体数を増やして確認する必要がある．採血管の種類に依らず共通して干渉作用のある項目は，遊離脂肪酸とリポプロテインの2項目であった．血液にDexを添加した検体でもリポプロテインの低下を認めるため，脂質粒子として血漿中に存在するリポプロテインが，Dex添加により凝集して一部が沈降することで低値となったものと考えられる．遊離脂肪酸は血液にHb小胞体とDexを共存させた検体でのみ増大し，血液にHb小胞体あるいは血液にDexを添加した検体では干渉を認めなかった．このことから，Hb小胞体にDexを添加することにより遊離脂肪酸が増大したと考えられ，遊離脂肪酸についてはDexを添加しない方が正確な測定値が得られている．

凝固線溶検査ではHb小胞体の存在によりATIIIで上昇，トータルPAI-1で低下を示し，その他FDP，D-ダイマーを除くすべての検査で測定不能と判断された（Table 4）．一方，Hb小胞体浮遊血液にDexを添加し遠心分離で除去した血漿では，vWF活性の低下とトータルPAI-1の上昇を除き干渉作用を回避できた．この2項目では，Hb小胞体の有無に依らず血液にDexを添加した場合にも同程度のvWF活性の低下とトータルPAI-1の上昇を認めることから，Dexの添加が干渉作用の原因と考えられる．これらの項目については他の方法を模索する必要がある．糖尿病関連検査に関してはグルコース，Hb_{A1C}ともにHb小胞体の影響を受けずに測定可能であった（Table 5）．本研究では，一回の測定であるが多くの項目でHb小胞体の干渉作用を回避できる効果が示された．生化学・免疫学検査や凝固線溶検査は人工酸素運搬体の安全性を評価する上でも重要な検査項目であり[25,26]，今後はこの方法で測定検体を増やし，統計的に信頼性を解析すると共に，Hb小胞体の投与が想定される各種病態における血液検体における評価も必要に応じて実施する必要がある．

4．結論

Hb小胞体が混在する血液検体では，通常の遠心により血液検査に適した血漿を得ることができず，多くの項目で測定が干渉される．一方，Dex（分子量400～500 kDa）の添加（終濃度; 2.6g/dl）により，従来通りの遠心で血清または血漿が得られる．

生化学・免疫学検査，凝固線溶検査，糖尿病関連検査の大部分の検査項目について干渉作用なく測定できることが確認され，Hb小胞体投与後の血液検体検査が容易になると考える．ただし，Dex添加の影響により生化学検査ではリポプロテイン（A）の低下，凝固検査ではvWF活性の低下，トータルPAI-1の上昇が見られているので，これらの項目については注意を要す．

謝辞

本研究は，厚生労働科学研究費補助金（医薬品・医療機器等レギュラトリーサイエンス総合研究事業）によって行われた．記して謝意を表す．

参考文献

1. Ma Z, Monk TG, Goodnough LT, McClellan A, Gawryl M, Clark T, Moreira P, Keipert PE, Scott MG. Effect of hemoglobin- and Perflubron-based oxygen carriers on common clinical laboratory tests. Clin Chem 1997;43:1732-1737.
2. Callas DD, Clark TL, Moreira PL, Lansden C, Gawryl MS, Kahn S, Bermes EW Jr. In vitro effects of a novel hemoglobin-based oxygen carrier on routine chemistry, therapeutic drug, coagulation, hematology, and blood bank assays. Clin Chem 1997;43:1744-1748.
3. Ali AC, Campbell JA. Interference of o-raffinose cross-linked hemoglobin with routine Hitachi 717 assays. Clin Chem 1997;43:1794-1796.
4. Alonsozana GL, Elfath MD, Mackenzie C, Gregory LC, Duh SH, Trump B, Christenson RH. In vitro interference of the red cell substitute pyridoxalated hemoglobin-polyoxyethylene with blood compatibility, coagulation, and clinical chemistry testing. J Cardiothorac Vasc Anesth 1997;11:845-850.
5. Kazmierczak SC, Catrou PG, Best AE, Sullivan SW, Briley KP. Multiple regression analysis of interference effects from a hemoglobin-based oxygen carrier solution. Clin Chem Lab Med 1999;37:453-64.
6. Wolthuis A, Peek D, Scholten R, Moreira P, Gawryl M, Clark T, Westerhuis L. Effect of the hemoglobin-based oxygen carrier HBOC-201 on laboratory instrumentation: cobas integra, chiron blood gas analyzer 840, Sysmex SE-9000 and BCT. Clin Chem Lab Med 1999;37:71-6.
7. Chance JJ, Norris EJ, Kroll MH. Mechanism of interference of a polymerized hemoglobin blood substitute in an alkaline phosphatase method. Clin Chem. 2000;46:1331-1337.
8. 酒井宏水，富山賢一，政田陽平，武岡真司，堀之内宏久，小林紘一，土田英俊．酸素輸液（ヘモグロビン小胞体）を含有する血清の生化学的検査．人工血液 2002;10:47-53.
9. Sakai H, Tomiyama K, Masada Y, Takeoka S, Horinouchi H, Kobayashi K, Tsuchida E. Pretreatment of serum containing hemoglobin vesicles (oxygen carriers) to prevent their interference in laboratory tests Clin Chem Lab Med 2003;41:222-231.
10. Jahr JS, Osgood S, Rothenberg SJ, Li QL, Butch AW, Gunther R, Cheung A, Driessen B. Lactate measurement interference by hemoglobin-based oxygen carriers (Oxyglobin, Hemopure, and Hemolink). Anesth Analg 2005;100:431-436.
11. Osgood SL, Jahr JS, Desai P, Tsukamoto J, Driessen B. Does methemoglobin from oxidized hemoglobin-based oxygen carrier (hemoglobin Glutamer-200) interfere with lactate measurement (YSI 2700 SELECT Biochemistry Analyzer)? Anesth Analg 2005;100:437-9.
12. Björkholm M, Fagrell B, Przybelski R, Winslow N, Young M, Winslow RM. A phase I single blind clinical trial of a new oxygen transport agent (MP4), human hemoglobin modified with maleimide-activated polyethylene glycol. Haematologica 2005;90:505-515.
13. Moon-Massat PF, Tierney JP, Hock KG, Scott MG. Hitachi Hemolytic Index correlates with HBOC-201 concentrations: impact on suppression of analyte results. Clin Biochem 2008;41:432-5.
14. Cameron SJ, Gerhardt G, Engelstad M, Young MA, Norris EJ, Sokoll LJ. Interference in clinical chemistry assays by the hemoglobin-based oxygen carrier, Hemospan ((R)). Clin Biochem 2009 (in press).
15. Ali AA, Ali GS, Steinke JM, Shepherd AP. Co-oximetry interference by hemoglobin-based blood substitutes. Anesth Analg 2001;92:863-9.
16. Shepherd AP, Steinke JM. CO-oximetry interference by perflubron emulsion: comparison of hemolyzing and nonhemolyzing instruments. Clin Chem 1998;44:2183-90.
17. Hughes GS, Francom SF, Antal EJ, Adams WJ, Locker PK, Yancey EP, Jacobs EE. Effects of a novel hemoglobin-based oxygen carrier on percent oxygen saturation as determined with arterial blood gas analysis and pulse oximetry. Ann Emerg Med 1996;27:164-9.
18. Lurie F, Driessen B, Jahr JS, Reynoso R, Gunther RA. Validity of arterial and mixed venous oxygen saturation measurements in a canine hemorrhage model after resuscitation with varying concentrations of hemoglobin-based oxygen carrier. Anesth Analg 2003;96:46-50
19. Chan FP, Jahr JS, Driessen B, Daunt DA, Li KC. Validation of in vivo MR measurement of oxygen saturation after resuscitation with a hemoglobin-based oxygen carrier in a rabbit model. Acad Radiol 2001;8:583-90.
20. 池田達彦，堀之内宏久，井澤菜緒子，泉陽太郎，河野光智，渡

辺真純, 川村雅文, 酒井宏水, 土田英俊, 小林紘一, Beagle犬を用いた50%脱血ショックにおけるHb小胞体の蘇生効果および酸素運搬能の評価, 第13回日本血液代替物学会アブストラクト, 人工血液 2006;14:21.
21. Sunamoto J, Iwamoto K, Kondo H, Shinkai S. Liposomal membranes. VI. Polysaccharide-induced aggregation of multilamellar liposomes of egg lecithin. J Biochem 1980;88:1219-26.
22. Meyuhas D, Nir S, Lichtenberg D. Aggregation of phospholipid vesicles by water-soluble polymers. Biophys J 1996;71:2602-12.
23. Takeoka S, Sou K, Arase S, Ohgushi T, Tsuchida E. Critical molecular weight effects in the aggregation of phospholipid vesicles triggered by water-soluble polymers and an integrated glycolipid. Macromolecules 1996;29:8132-8136.
24. Sakai H, Sato A, Takeoka S, Tsuchida E. Rheological properties of hemoglobin vesicles (artificial oxygen carriers) suspended in a series of plasma-substitute solutions. Langmuir 2007;17:23:8121-8.
25. 高折益彦. 人工血液としての条件liposome-encapsulated hemoglobinの有効性, 安全性への検討. 人工血液 2002;10:28-35.
26. 高折益彦. 酸素運搬体の臨床治験へ. 人工血液 2004;12:67-73.

Hemoglobin-vesicle, a cellular artificial oxygen carrier, that fulfils the physiological roles of the red blood cells structure

Hiromi Sakai[1]*, Keitaro Sou[1], Hirohisa Horinouchi[2], Koichi Kobayashi[2], and Eishun Tsuchida[1]

[1]Research Institute for Science and Engineering, Waseda University, Tokyo, Japan;
[2]Department of Surgery, School of Medicine, Keio University, Tokyo, Japan.
*Corresponding Author: Hiromi Sakai, Associate Professor, Research Institute for Science and Engineering, Waseda University, Tokyo 169-8555, Japan, Tel: +81-3-5286-3122, Fax: +81-3-3205-4740, E-mail: hiromi@waseda.jp

Abstract Hb-vesicles (HbV) are artificial O_2 carriers encapsulating concentrated Hb solution (35 g/dL) with a phospholipid bilayer membrane (liposome). The concentration of the HbV suspension is extremely high ([Hb] = 10 g/dL) and it has an O_2 carrying capacity that is comparable to that of blood. HbV is much smaller than RBC (250 vs. 8000 nm), but it recreates the functions of RBCs; (i) the slower rate of O_2 unloading than Hb solution; (ii) colloid osmotic pressure is zero; (iii) the viscosity of a HbV suspension is adjustable to that of blood; (iv) HbV is finally captured by and degraded in RES; (v) co-encapsulation of an allosteric effector to regulate O_2 affinity; (vi) the lipid bilayer membrane prevents direct contact of Hb and vasculature; (vii) NO-binding is retarded to some extent by an intracellular diffusion barrier, and HbV does not induce vasoconstriction. (viii) Both RBC and HbV can be a carrier of not only O_2 but also exogenous CO. However, HbV has limitations such as a shorter functional half-life when compared with RBCs. On the other hand, the advantages of HbV are that it is pathogen-free and blood-type-antigen-free; moreover, it can withstand long-term storage of a few years, none of which can be achieved by the RBC transfusion systems.

1 Introduction

Biconcave RBCs deform to a parachute-like configuration to flow through a narrower capillary. This profile is believed to be effective to increase the surface-to-volume ratio and stir the intracellular viscous Hb solution to facilitate the gas exchange. On the other hand, physicochemical analyses have revealed that O_2 unloading of Hb is significantly retarded by compartmentalization in RBC. Why has

nature selected such an inefficient cellular structure for gas transport? Interestingly, some of the answers to this question have been revised by the research of blood substitutes. They are, (i) retardation and targeting of O_2 unloading at microcirculation to avoid autoregulatory vasoconstriction; (ii) reduction of a high colloidal osmotic pressure, COP, of an Hb solution to zero, to increase blood Hb concentration; (iii) rheology control of blood, a RBCs dispersion, to a non-Newtonian viscous fluid; (iv) prevention of extravasation or excretion through renal glomeruli; (v) preservation of the chemical environment in cells, such as the concentrations of electrolytes and enzymes; (vi) prevention of direct contact of toxic Hbs and endothelial cell lying, and (vii) modulation of reactions with NO as an endothelium derived relaxation factor, EDRF. These observations reassure the importance of the cellular structure of RBCs to design Hb-based oxygen carriers.

Hb-vesicles (HbV) are artificial O_2 carriers encapsulating concentrated Hb solution (35 g/dL) with a phospholipid bilayer membrane [1]. Concentration of the HbV suspension is extremely high ([Hb] = 10 g/dL, [lipids] = 6 g/dL, volume fraction, ca. 40 vol%) and it has an oxygen carrying capacity that is comparable to that of blood. In this review paper, we summarize the characteristics of HbV that can fulfill some of the physiological roles of the cellular RBC structure.

2 Structural stability and suspension properties

Many people think liposomes are unstable capsules. However, it depends on the lipids and the composition. In the case of RBCs, the sophisticated cytoskeleton network structure stabilizes the cellular structure. However, hypotonic hemolysis easily occurs. We confirmed that HbV are more resistant than RBCs to hypotonic shock, freezing by liquid N_2 and thawing, enzymatic attack (phospholipase A_2) [2], and a shear stress (1500 s^{-1}). Moreover, it can be stored at room temperature over two years [3]. In spite of such high stability, we confirmed with animal experiments that HbV are eventually captured by reticuloendothelial system (RES) and degraded promptly within 2 weeks without decomposing (hemolysis) in blood circulation [4]. Phospholipid vesicles for the encapsulation of Hb would be beneficial for heme detoxification through their preferential delivery to the RES, a physiological compartment for degradation of senescent RBCs, even at doses greater than putative clinical doses [5].

Colloid osmotic pressure (COP) is an important factor to determine blood volume in the body. Hb solution (5 g/dL) showed the COP of 16 Torr [6]. Polymerization of Hb reduces COP depending on the resulting molecular weight. PEG-conjugated Hb shows the largest COP, which is about 3 times higher than blood (ca. 25 Torr) due to the highly hydrated PEG chains [7]. On the other hand, both HbV and washed RBCs showed 0 Torr because of the suspension of large particles: the number of total particles of HbV is less than 1/100 of the number of Hb molecules at the same Hb concentration [6]. COP acts in opposition to hydrostatic

pressure to balance the distribution of fluid between blood and interstitial compartments [7]. COP is a colligative property, depending proportionally on the concentration of protein exerting the force and specifically on the macromolecular properties of that protein. Solutions with high COP cause significant transcapillary filtration of water in the direction from the interstitial space into the vascular lumen. An increase in blood volume is advantageous to increase cardiac output for resuscitation, though the composition of other components of blood and tissue will also be compromised. HbV, on the other hand, does not have an oncotic effect, and the particle should be suspended in a plasma expander (plasma substitute, water-soluble polymer). The COP of the resulting suspension is identical to that of the suspending medium. When HbV is suspended in 5% rHSA, the suspension shows 20 Torr at any Hb concentration. HbV can create a suspension of [Hb] = 10 g/dL at the physiologic COP, that cannot be attained easily by other chemically modified Hb solutions.

The HbV suspended in rHSA ([Hb] = 10 g/dL) was nearly Newtonian [8]. Other plasma substitute polymers -hydroxylethyl starch (HES), dextran (DEX), and modified fluid gelatin (MFG)- induced HbV flocculation, possibly by depletion interaction, and rendered the suspensions as non-Newtonian with a shear-thinning profile. These HbV suspensions showed a high storage modulus (G') because of the presence of flocculated HbV. However, HbV suspended in rHSA exhibited a very low G'. The viscosities of HbV suspended in DEX, MFG, and high-molecular-weight HES solutions responded quickly to rapid step changes in shear rates of 0.1-100 s^{-1} and a return to 0.1 s^{-1}, indicating that flocculation is both rapid and reversible. The HbV suspension viscosity was influenced by the presence of plasma substitutes. The HbV suspension provides a unique opportunity to manipulate rheological properties for various clinical applications.

3 The rate of O_2-unloading, and NO- and CO-bindings

The O_2-release from flowing HbVs was examined using an O_2-permeable, fluorinated ethylenepropylene copolymer tube (inner diameter, 28 μm) exposed to a deoxygenated environment [9]. Measurement of O_2 release was performed using an apparatus that consisted of an inverted microscope and a spectrophotometer, and the rate of O_2 release was determined based on the visible absorption spectrum in the *Q* band of Hb. HbVs and human RBCs were mixed in various volume ratios at [Hb] = 10 g/dl, and the suspension was perfused at the centerline flow velocity of 1 mm/s through the narrow tube. The mixtures of cell-free Hb solution and RBCs were also tested. Because HbVs were homogeneously dispersed, increasing the volume of the HbV suspension resulted in a thicker marginal RBC-free layer. Irrespective of the mixing ratio, the rate of O_2 release from the HbV/RBC mixtures was similar to that of RBCs alone. On the other hand, the addition of 50 vol% of acellular Hb solution to RBCs significantly enhanced the rate of deoxygenation.

This difference between the HbV suspension and the acellular Hb solution should mainly be due to the difference in the particle size (250 vs. 7 nm) that affects their diffusion for the facilitated O_2 transport. It has been suggested that faster O_2 unloading from the HBOCs is advantageous for tissue oxygenation. However, this concept is controversial with regard to the recent findings, because an excess O_2 supply would cause autoregulatory vasoconstriction and microcirculatory disorders. We confirmed that HbVs do not induce vasoconstriction and hypertension. This is not only owing to the reduced inactivation of NO (see below) but also possibly due to the moderate O_2 release rate that is similar to RBCs.

One of the important roles of the RBC structure is the retardation of NO-binding. However, the mechanism has been controversial, whether, (i) an unstirred layer surrounding the cell should be the diffusion barrier, (ii) cytoskeletal cell membrane can be the diffusion barrier, or (iii) the highly concentrated Hb solution can be the barrier. To clarify the mechanism, we analyzed HbVs with different intracellular Hb concentrations, $[Hb]_{in}$, and different particle sizes using stopped-flow spectrophotometry [10]. In the case of different $[Hb]_{in}$ (1- 35 g/dl), NO-binding is retarded at a higher $[Hb]_{in}$, on the other hand, CO-binding did not show such retardation. In the case of different particle diameter of HbV at constant $[Hb]_{in}$, 35 g/dl, NO-binding is retarded with a larger particle, while the CO-binding did not show such changes. The computer simulations can recreate these tendencies. The two-dimensional concentration changes of free-NO and unbound free-hemes in one HbV at the $[Hb]_{in}$ was 1 g/dl showed that NO diffuses rapidly into HbV and the reaction proceeds quite homogeneously. On the other hand, HbV at $[Hb]_{in}$ = 35g/dl showed heterogeneous distribution. The concentration gradients of both NO and heme change from the interior surface to the core. The intrinsically fast NO-binding induces an intracellular diffusion barrier in a highly concentrated Hb solution, but not for the slow CO-binding. We can estimate the apparent binding rate constant of a particle encapsulating a 35-g/dl Hb with 8000-nm diameter, and they are similar to the reported values for RBCs. The mechanism of retardation of NO-binding is controversial, but from these data, we estimate that (i) rapid NO-binding reaction induces intracellular diffusion barrier, (ii) cellular membrane cannot be a barrier for gas diffusion, and (iii) a higher $[Hb]_{in}$ and larger size are the factors for retarding NO-binding. However, we have to admit that NO-binding of HbV is much faster than that of RBC. The absence of vasoconstriction for HbV cannot be explained with these data. We believe that small Hb would permeate across the endothelium to reach to the site where NO is produced and transferred to the smooth muscle. It was recently reported that dextran conjugated Hb permeates through the endothelium. However, much larger HbV would remain in the lumen and does not bind NO in the endothelium.

4 Resuscitation from hemorrhagic shock with HbV

The first attempt of HbV to restore the systemic condition after hemorrhagic shock was conducted using anesthetized Wistar rats. After 50% blood withdrawal, the rats showed hypotension and considerable metabolic acidosis and hyperventilation. They received HbV suspended in rHSA, shed autologous blood (SAB), or rHSA alone. The HbV group restored mean arterial pressure, similar to the SAB group, which was significantly higher than the rHSA group. No remarkable difference was visible in the blood gas variables between the resuscitated groups. However, two of eight rats in the rHSA group died before 6 h [11]. After removing the catheters and awakening, the rats were housed in cages for up to 14 days. The HbV group gained body weight; the reduced Hct returned to the original level in 7 days, indicating elevated hematopoiesis. Both groups showed transient elevation of AST and ALT at 1 day. Splenomegaly was significant in the HbV group at 3 days because of the accumulation of HbV. However, it subsided within 14 days. Histopathological observation indicated that a significant amount of HbV accumulated in the spleen macrophages, and complete disappearance within 14 days. These results indicate that HbV is useful as a resuscitative fluid for hemorrhagic shock. Its performance is comparable to that of SAB. Similar experiments using beagles have shown one-year survival after resuscitation with HbV.

The above elevations of AST and ALT after resuscitation with HbV or RBC indicate the systemic reperfusion injury. Recent reports on cytoprotective effects of exogenous CO urged us to test infusion of CO-bound HbV and RBC in hemorrhagic-shocked rats to improve tissue viability [12]. Using the similar model, hemorrhagic shocked Wistar rats received CO-HbV, CO-RBC, O_2-HbV, or O_2-RBC suspended in 5% rHSA. All groups showed prompt recovery of blood pressure and blood gas parameters, and survived for 6 h of observation period. Plasma AST, ALT and LDH levels were elevated at 6 h in the O_2-HbV and O_2-RBC groups. They were significantly lower in the CO-HbV and CO-RBC groups. Blood HbCO levels (26–39%) decreased to less than 3% at 6 h while CO was exhaled through the lung. Both HbV and RBC gradually gained the O_2 transport function. Collectively, both CO-HbV and CO-RBC showed a resuscitative effect and reduced oxidative damage to organs. Adverse and poisonous effects of CO gas were not evident for 6 h in this experimental model. Further study is necessary to clarify the neurological impact of a longer observation period, though the results suggest a possible new clinical indication.

In conclusion, HbV can mimic the functions of RBCs. However, the half-life of HbV is much shorter than that of RBCs, and limits their use. On the other hand, the advantages of HbV are that it is pathogen-free and blood-type-antigen-free; moreover, it can withstand long-term storage of a few years, none of which can be achieved by the RBC transfusion systems. We continue further development of HbV aiming at the eventual realization and contribution to the clinical medicine.

Acknowledgments This work is supported by Health and Labour Sciences Research Grants (Health Science Research Including Drug Innovation), Ministry of Health, Labour and Welfare, Japan (H.S. H.H, E.T, K.K.), and Grants in Aid for Scientific Research from the Japan Society for the Promotion of Science (B19300164) (H.S.).

References

[1] Sakai H, Sou K, Horinouchi H, Kobayashi K, Tsuchida E. (2008) Haemoglobin-vesicles as artificial oxygen carriers: present situation and future visions. J Intern Med 263:4-15.

[2] Sakai H, Okamoto M, Ikeda E, Horinouchi H, Kobayashi K, Tsuchida E. (2009) J Biomed Mater Res A (in press).

[3] Sakai H, Tomiyama KI, Sou K, Takeoka S, Tsuchida E. (2000) Poly(ethylene glycol)-conjugation and deoxygenation enable long-term preservation of hemoglobin-vesicles as oxygen carriers in a liquid state. Bioconjug Chem 11:425-432

[4] Sakai H, Horinouchi H, Tomiyama K, Ikeda E, Takeoka S, Kobayashi K, Tsuchida E. (2001) Hemoglobin-vesicles as oxygen carriers: influence on phagocytic activity and histopathological changes in reticuloendothelial system. Am J Pathol 159:1079-1088.

[5] Sakai H, Masada Y, Horinouchi H, Ikeda E, Sou K, Takeoka S, Suematsu M, Takaori M, Kobayashi K, Tsuchida E. (2004) Physiological capacity of the reticuloendothelial system for the degradation of hemoglobin vesicles (artificial oxygen carriers) after massive intravenous doses by daily repeated infusions for 14 days. J Pharmacol Exp Ther 311:874-884.

[6] Sakai H, Yuasa M, Onuma H, Takeoka S, Tsuchida E. (2000) Synthesis and physicochemical characterization of a series of hemoglobin-based oxygen carriers: objective comparison between cellular and acellular types. Bioconjug Chem 11:56-64.

[7] Vandegriff KD, McCarthy M, Rohlfs RJ, Winslow RM. (1997) Colloid osmotic properties of modified hemoglobins: chemically cross-linked versus polyethylene glycol surface-conjugated. Biophys Chem 69:23-30.

[8] Sakai H, Sato A, Takeoka S, Tsuchida E. (2007) Rheological properties of hemoglobin vesicles (artificial oxygen carriers) suspended in a series of plasma-substitute solutions. Langmuir 23:8121-8128.

[9] Sakai H, Suzuki Y, Kinoshita M, Takeoka S, Maeda N, Tsuchida E. (2003) O_2 release from Hb vesicles evaluated using an artificial, narrow O_2-permeable tube: comparison with RBCs and acellular Hbs. Am J Physiol Heart Circ Physiol 285:H2543-H2551

[10] Sakai H, Sato A, Masuda K, Takeoka S, Tsuchida E. (2008) Encapsulation of concentrated hemoglobin solution in phospholipid vesicles retards the reaction with NO, but not CO, by intracellular diffusion barrier. J Biol Chem 283:1508-1517

[11] Sakai H, Masada Y, Horinouchi H, Yamamoto M, Ikeda E, Takeoka S, Kobayashi K, Tsuchida E. (2004) Hemoglobin-vesicles suspended in recombinant human serum albumin for resuscitation from hemorrhagic shock in anesthetized rats. Crit Care Med 32:539-545.

[12] Sakai H, Horinouchi H, Tsuchida E, Kobayashi K. (2009) Hemoglobin-vesicles and red blood cells as carriers of carbon monoxide prior to oxygen for resuscitation from hemorrhagic shock in a rat model. Shock (in press).

Static Structures and Dynamics of Hemoglobin Vesicle (HbV) Developed as a Transfusion Alternative

Takaaki Sato,[†,‡] Hiromi Sakai,[*,‡] Keitaro Sou,[‡] Martin Medebach,[§]

Otto Glatter,[§] and Eishun Tsuchida[*,‡]

[†]International Young Researchers Empowerment Center, Shinshu University, Tokida 3-15-1, Ueda 386-8567, Japan, [‡]Research Institute for Science and Engineering, Waseda University, Okubo 3-4-1, Shinjuku-ku, Tokyo 169-8555, Japan, [§]Physical Chemistry, Institute of Chemistry, University of Graz, Graz A-8010, Austria

AUTHOR EMAIL ADDRESS: hiromi@waseda.jp, eishun@waseda.jp

*To whom correspondence should be addressed. E-mail: hiromi@waseda.jp, eishun@waseda.jp.

Phone: +81-3-5286-3122. Fax: +81-3-3205-4740

ABSTRACT Hemoglobin vesicle (HbV) is an artificial oxygen carrier that encapsulates solution of purified and highly concentrated (ca. 38 g dL^{-1}) human hemoglobin. Its exceptionally high concentration as a liposomal product (ca. 40% volume fraction) achieves an oxygen-carrying capacity comparable to that of blood. We use small-angle X-ray scattering (SAXS) and dynamic light scattering (DLS) to investigate the hierarchical structures and dynamics of HbVs in concentrated suspensions. SAXS data revealed uni-lamellar shell structure and internal density profile of the artificial cell membrane for Hb encapsulation. The SAXS intensity of HbV at scattering vector $q > 0.5$ nm^{-1} manifests dissolution states of the encapsulated Hbs in the inner aqueous phase of the vesicle having ca. 240 nm diameter. The peak position as well as the height and width of static structure factor of Hb before and after encapsulation are almost identical, demonstrating the preserved protein-protein interactions in the confined space. To overcome multiple scattering from turbid samples, we employed thin layer-cell DLS combined with the so-called bruteforce and echo techniques, which allows us to observe collective diffusion dynamics of HbVs without dilution. A pronounced slowdown of the HbV diffusion and eventual emergence of dynamically arrested state in the presence of high-concentration plasma substitutes (water-soluble polymers), such as dextran, modified fluid gelatin, and hydroxylethyl starch, can be explained by depletion interaction. A significantly weaker effect of recombinant human serum albumin on HbV flocculation and viscosity enhancement than those induced by other polymers is clearly attributed to the specificity as a protein; its compact structure efficiently reduces the reservoir polymer volume fraction that determines the depth of the attractive potential between HbVs. These phenomena are technically essential for controlling the suspension rheology, which is advantageous for versatile clinical applications.

KEYWORDS: Hemoglobin vesicle (HbV), transfusion alternative, phospholipid bilayer membrane, small-angle X-ray scattering (SAXS), dynamic light scattering (DLS)

Introduction

Phospholipid vesicles, often called liposomes, encapsulating or embedding functional drugs, have long been investigated for their practical use as drug-delivery systems. They in part have already been approved for antifungal or anticancer therapy.[1] Hemoglobin vesicle (HbV), or liposome encapsulated Hb, is an artificial oxygen carrier that encapsulates a purified and highly concentrated Hb solution in a phospholipid vesicle.[2-7] The safety and an oxygen-carrying capacity of HbV as a transfusion alternative have enthusiastically been evaluated in animal tests.[7-9] Its exceptionally high concentration ([Hb] = 10 g dL^{-1}; [lipids] = ca. 6 g dL^{-1}) compared to any other conventional liposomal products offers sufficient oxygen-carrying capacity comparable to that of blood. HbVs are now widening their uses, aimed at other novel clinical applications, such as the oxygenation of ischemic tissues and the ex vivo perfusion system.[10]

Physiological significance of the cellular structure of the red blood cell (RBC) is underlined by the retardation of entrapment of endogenous vasorelaxation factors (NO and CO),[11,12] preservation of chemical environments, screening of high colloid osmotic pressure (COP) of a concentrated Hb solution, and so forth. By mimicking RBCs, HbV is equipped with the hierarchically organized cellular structures despite its far smaller size.[2,3,7-9] Owing to this notable feature, serious side effects of molecular Hb that causes strong vasoconstriction can be avoided.[13,14] Successful fabrication of the HbV fine particle was previously confirmed by indirect mathematical calculation of lamellarity and intracellular Hb concentration using the particle size and the total concentrations of the components in a dispersion, or microscopic observation of a dried sample.[15,16] However, statistically valid, full structural characterization of HbV in a dispersion state remains to be done. In particular, microscopic internal structures of the phosphorlipid bilayer membrane whose composition is precisely optimized for Hb encapsulation and long-term preservation, and the dissolution state of the concentrated Hbs confined into the inner aqueous phase of the vesicle are of great interest. To access such structural details, we used small-angle x-ray scattering (SAXS).[17,18]

On the one hand, the preservation or adjustment of COP is one of the important requirements for a transfusion alternative to sustain the blood circulation. In the human body, human serum albumin (HSA), most abundant plasma protein in our blood stream (dissolved at ca. 5 g dL^{-1}), preserves COP of blood (ca. 20 Torr).[19] Since HbV suspended in saline solution does not contribute to COP of blood, HbV must be co-injected with solution of HSA or other plasma substitutes (water soluble polymers) for its clinical use. However, an addition of nonadsorbing polymers to a suspension of colloidal particles generally induces an aggregation tendency of colloidal particles, as known to occur for various particle systems, such as polystyrene beads, silica, liposomes, and RBCs.[20-25] At high enough polymer volume fraction, it

often causes phase separation. A theoretical description on this intriguing phenomenon was first given by Asakura and Oosawa;[26,27] exclusion or depletion of small particles or polymer molecules from the region closely spaced large colloid particles lead to an effective attractive potential between the two large particles, increasing the overall disorder.[26-31] This entropic driven force is of fundamental importance as well as technologically implicative, as highlighted by the practical use of nonadsorbing polymers as rheological modifiers for colloidal products. This is indeed valid for medical applications of HbVs; as we have shown, the combination of HbV and different plasma substitute solutions provide an opportunity to manipulate the suspension rheology.[32,33]

From a physiological and medical point of view, high viscosity fluid is often advantageous for sustaining peripheral blood flow, giving shear stress on the vascular wall to facilitate the production of vasorelaxation factors, such as nitric oxide and prostacyclin.[32-36] The HbV suspended in solution of recombinant HSA (rHSA) behave nearly as a Newtonian fluid,[3,32,38] whereas other polymers, such as hydroxylethyl starch (HES), dextran (DEX), and modified fluid gelatin (MFG) medically used worldwide in medical treatments,[39-41] lead to non-Newtonian nature and hyperviscosity.[32] This is possibly due to HbV flocculation induced by depletion interaction. To gain deeper insights into the underlying mechanism, we used thin layer-cell dynamic light scattering (TC-DLS)[42,43] combined with bruteforce[44] and echo[43-45] techniques. This enables us to observe collective diffusion in a concentrated HbV suspension and its mixtures with plasma substitutes without dilution, overcoming the interference from multiple scattering of turbid samples. The results are not only implicative in interdisciplinary fields of soft-condensed matter physics and bio-chemistry, but of practical importance for a new class of forthcoming medical applications.

Experimental section

Materials. The HbV was prepared under sterile conditions, according to the previously reported procedures.[15,46,47] Hbs are purified from outdated donated blood provided by the Japanese Red Cross Society (Tokyo, Japan). The Hb solutions for encapsulation were prepared from this stock solution by adjusting the concentration to 38 g dL^{-1}. The encapsulated purified Hb contained 14.7 mM pyridoxal 5'-phosphate (PLP; Sigma) as an allosteric effector in a molar ratio of PLP/Hb = 2.5. The lipid bilayer membrane for the Hb encapsulation comprises 1,2-dipalmitoyl-*sn*-glycero-3-phosphatidylcholine, cholesterol, and 1,5-bis-*O*-hexadecyl-*N*-succinyl-L-glutamate, mixed in the molar ratio of 5/5/1 (Nippon Fine Chemical Co. Ltd., Osaka, Japan) and 1,2-distearoyl-*sn*-glycero-3-phosphatidylethanolamine-*N*-poly(ethylene glycol) (NOF Corp., Tokyo, Japan) at 0.3 mol% of the total lipid. The HbVs were suspended in a physiologic saline solution at [Hb] = 10 g dL^{-1} ([lipids] = ca. 6 g dL^{-1}) and were deoxygenated for storage with N_2 bubbling in vials.[48]

The plasma substitutes used in this study are listed in Table 1. Recombinant human serum albumin (rHSA, M_w = 67 kDa, 25 g dL^{-1}) was a gift from Nipro Corp. (Osaka, Japan). A dextran (DEX) solution (M_w = 40 kDa, 10 g dL^{-1} in a physiological saline solution) was purchased from Kobayashi Pharmaceutical Co. Ltd. (Osaka, Japan). Solutions of hydroxylethyl starch (HES) with different molecular weights were assorted; an HES_{70} solution (Saline-HES, M_w = 68 kDa, 6 g dL^{-1} in a physiological saline solution) was purchased from Kyorin Pharmaceutical Co. Ltd. (Osaka, Japan). An HES_{130} solution (Voluven, M_w = 130 kDa, 6 g dL^{-1} in a physiological saline solution) was a gift from Fresenius Kabi AG (Homburg v.d.H., Germany). An HES_{670} solution (Hextend, M_w = 670 kDa, 6 g dL^{-1} in a physiological Ringer lactate solution) was obtained from Hospira, Inc. (Lake Forest, IL). A modified fluid gelatin (MFG) solution (Gelofusin, M_w = 30 kDa, 4 g dL^{-1} in a physiological saline solution) was a gift from B. Braun Melsungen AG (Melsungen, Germany). As a standard for testing the accuracy of our dynamic light scattering (DLS) experiments, a pseudo-monodisperse microsphere with a nominal diameter of 0.209 μm with a 0.011 μm standard deviation (Polyscences, Inc., USA) was used.

For optimized experimental conditions, the concentration of the HbV dispersions was further adjusted for small-angle X-ray scattering (SAXS) and dynamic light scattering (DLS) experiments by adding a saline solution (Otsuka Pharmaceutical Co. Ltd., Osaka, Japan) or solutions of plasma substitute, and these samples were immediately used for experiments.

Small-angle X-ray scattering (SAXS). We performed SAXS measurements on HbV suspensions and their model systems to examine their static structures. We used a SAXSess camera (Anton-Paar, Graz, Austria) attached to a PW3830 sealed-tube anode X-ray generator (PANalytical, Netherlands). The generator was operated at 40 kV and 50 mA. A Göbel mirror and a block collimator provide a focused monochromatic X-ray beam of Cu-K_α radiation (λ = 0.1542 nm) with a well-defined shape. A thermostated sample holder unit (TCS 120, Anton Paar) was used to control the sample temperature. The 2D scattering patterns recorded by an imaging-plate (IP) detector (a Cyclone, Perkin Elmer, USA) were integrated into to one-dimensional scattered intensities $I(q)$ as a function of the magnitude of the scattering vector $q = (4\pi/\lambda)\sin(\theta/2)$ using SAXSQuant software (Anton Paar), where θ is the total scattering angle. For all experiments, we monitored attenuated primary beam at $q = 0$ using a semi-transparent beam stop. All the measured intensities were semi-automatically calibrated for transmission by normalizing a zero-q primary intensity to unity. The background scattering contributions from capillary and solvent were corrected. The absolute intensity calibration was made by using water intensity as a secondary standard.[49]

Dynamic light scattering (DLS). We used dynamic light scattering (DLS) to study the size and size distribution using a laboratory-built goniometer, equipped with single-mode fiber optics and an ALV single-photon detector (ALV-Laser Vertriebsgesellschaft, Langen, Germany) for detection of a

time-dependent scattered intensity. A 8-mm cylindrical sample cell was immersed in a temperature-controlled index match bath filled with decalin solvent. The light source was a Verdi V5 diode laser from Coherent, with a wavelength of 532 nm with a maximum output of 5 W. The data acquisition was performed with an ALV 5000 multiple tau-digital correlator. The ALV-5000/E software package was used to calculate the intensity time-correlation functions.

Thin-layer cell dynamic light scattering (TC-DLS). In order to overcome the problems of multiple scattering from turbid samples caused by typically sub-micron particle size and their high concentration, we used a modified thin-layer cell dynamic light-scattering (TC-DLS) technique.[42,43] The TC-DLS apparatus was constructed based on an apparatus originally designed for static light scattering (SLS) on turbid colloidal dispersions,[50,51] which was equipped with a flat cell with variable thickness of 15, 50 and 100 μm, a single-mode fiber, and the ALV-5000 correlator (ALV-Laser GmbH, Langen Germany) for autocorrelation measurements of the time-dependent scattered light intensity via the fiber and the photomultiplier. A 10mW HeNe laser with a wavelength of 632.8 nm was used as a light source. The current setting allows the measurements of the scattered light between 15° and 45°.

Bruteforce and echo DLS experiments for arrested media. We used brute-force ensemble averaging technique[44] in combination with echo DLS[43-45] in the TC configuration to achieve a multi-speckle observation. The method allows us to pursuit arrested slow dynamics of the HbV particles in flocculation in the presence of a kind of plasma substitute. Under the condition that an ergodicity assumption is violated, that is, when equivalence of time-averaging with ensemble-averaging is not fulfilled, conventional DLS approaches based on a time-averaging of the intensity fluctuations of a single speckle become no longer valid. In order to achieve a proper ensemble averaging, we used for short time correlation times, the brute-force ensemble averaging, in which we monitored intensity fluctuations from many independent speckles, performing repeated short-time measurements for several hundreds of different sample cell configurations. For the measurements of the long-time tail of intensity correlation functions in the correlation time range of $\tau > 10$ sec, we used echo technique; if the intensity correlation function is measured with the sample cell precisely rotated, it allows to explore many independent sample configuration during one evolution of the rotation, avoiding a significantly longer time-averaging. In such an experiment, the ensemble averaged correlation function can be measured with relatively short averaging time. The echo peaks appear at multiples of $1/f$, where f is the frequency of the rotation, and the peak height slowly decays, reflecting the slow dynamics of the particles.

Table 1. Plasma Substitute Solutions and Their Physicochemical properties.

Plasma substitute	M_w (kDa)	c (g dL^{-1})	COP (Torr)	R_g (nm)

rHSA	67	5.0	19	2.84 [a]
HES_{70}	68	6.0	34	5.96 [a]
HES_{130}	130	6.0	35	6.83 [a]
HES_{670}	670	6.0	27	12.95 [a]
DEX	40	10.0	44	4.96 [a]
MFG	30	4.0	44	5.50 [a]

rHSA, recombinant human serum albumin; DEX, dextran; HES, hydroxyethyl starch; MFG, modified fluid gelatin; COP, colloid osmotic pressure. [a]R_g for plasma substitutes except rHSA was obtained with Guinier plot of SAXS data obtained at c = 1g dL^{-1}, and that for rHSA was calculated by using Guinier plot[17] against the form factor $P(q)$ obtained as an output of GIFT[52-54] procedure for c = 1g dL^{-1}.

Results and Discussions

Particle characterization of HbV in a dilute dispersion. The intensity autocorrelation function, $g_2(t)$, measured in the homodyne mode is connected to the normalized field correlation function, or the dynamic structure factor (DSF), $g_1(t)$, via the relation

$$g_2(t) = 1 + \beta |g_1(t)|^2 \quad (1)$$

where β is called coherence factor. The present experimental setup using single-mode fiber detection attains nearly its theoretical maximum of $\beta \sim 1$. In Figure 1, we present particle characterization of the HbV in a dilute dispersion ([Hb] + [Lipids] = 0.01 g dL^{-1}) as obtained by DLS. The effects of structure factor, $S(q)$, as well as hydrodynamic function, $H(q)$, are expected to be negligible at such low concentration. As a control, we tested pseudo-monodisperse microsphere with a nominal diameter of 0.209 μm (Polysciences, Inc., USA) to check the accuracy and the experimental broadening of our DLS experiments. Monodisperse spherical particles exhibits a single-exponential decay of $g_1(t)$

$$g_1(t) = \exp(-Dq^2 t) \quad (2)$$

where the D is the diffusion constant. D can be related to the hydrodynamic radius R_H of the hardsphere via the Stokes-Einstein relation

$$D = \frac{k_B T}{6\pi\eta R_H} \quad (3)$$

where k_B is Boltzmann constant, T is temperature, and η is solvent viscosity. The intensity correlation functions, $g_2(t)$, of both diluted dispersions of the HbV and the microsphere exhibit single-step relaxation behavior and a rapid convergence to the baseline (unity). For particle systems having a rather narrow size distribution that typically show single-step relaxation behavior, the second-order cumulant analysis[55] is often employed. The technique can be used as a convenient and fast method for obtaining a

semi-quantitative measure of the mean size and the width of its distribution. In Figure 2b, we display the cumulant plot, namely, a natural logarithm of the field correlation function, ln[$g_1(t)$], of the same DLS data shown in Figure 2a. Despite a smaller intercept for the HbV ($\beta \sim 0.85$), which is probably due to absorption of the hemoprotein, the slower decay of $g_1(t)$ for the HbV reflecting larger averaged size is apparent in this plot. The $g_1(t)$ of the microsphere shows almost ideal linear behavior up to its long-time tail, indicating a quite narrow relaxation time distribution, whereas that of HbV represents still small but clear deviation from the straight line at large τ, implying wider relaxation time distribution due to its size distribution. The cumulant analysis yielded R_H = 143 nm and 34.8% width of size distribution for HbV, and R_H =107 nm and 6.6% width for the pseudo-monodisperse microsphere

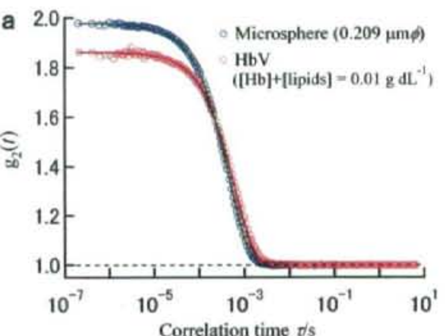

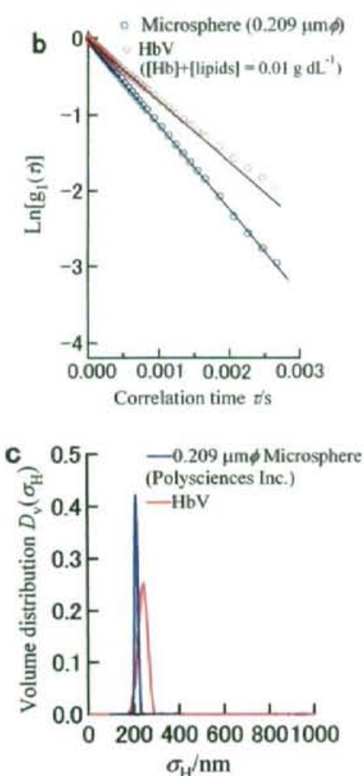

Figure 1: The particle characterization of HbV in a dilute dispersion as obtained by DLS. Intensity correlation functions, $g_2(t)$, of a dilute HbV dispersion ([Hb] = 6.3×10^{-3} g dL^{-1}) and a 0.027 wt% dispersion of pseudo-monodisperse microsphere with a nominal averaged diameter of 0.209 μm measured at 25 °C (a), the cumulant fit to the same DLS data (b), and the particle size distribution of the HbV and the microsphere, obtained by using optimized regularization technique (ORT).[56]

For further quantitative discussion, we also carried out a more detailed mathematical analysis. We evaluated the size-distributions by using optimized regularization technique (ORT),[56] which relies on

(indirect) inverse Laplace transformation of the experimental field correlation function, $g_1(t)$, into the relaxation-rate distribution functions. Assuming a linear combination of single exponential functions, $g_1(t)$ of polydisperse systems may be given by

$$g_1(t)=\int_{-\infty}^{\infty} G(\Gamma)\exp(-\Gamma t)\mathrm{d}\Gamma \quad (4)$$

The exponent Γ is proportional to the diffusion constant D as $\Gamma=Dq^2$. For the actual ORT evaluation, eq.(4) is replaced with

$$g_1(t)=\int_{-\infty}^{\infty} D(\tau)W(\tau)\exp(-t/\tau)/\tau^2\mathrm{d}\tau \quad (5)$$

where $D(\tau)$ is the distribution function, $W(\tau)$ is the weighting function, and $\Gamma = 1/\tau$. $W(\tau) = 1$ gives intensity distribution, and for volume or mass distribution, $W(\tau) = \tau^3$. We present the deduced volume distribution function of hydrodynamic diameter $D_V(\sigma_H)$, where $\sigma_H = 2R_H$. The ORT analysis provided a spike-like size distribution for the microsphere, which confirms negligibly small experimental broadening of our DLS experiments for the present purpose. The analysis on the HbV dispersion yielded an averaged hydrodynamic diameter, σ_H, of 238 nm and a narrow size distribution with a 20 nm standard deviation in the volume distribution. The data demonstrate well controlled geometry of the HbV particles as molecular assembly.

Structural characterization of the phospholipid bilayer membrane for Hb encapsulation. Figure 2 shows the X-ray scattered intensities $I(q)$ for a 6 g dL^{-1} dispersion of the vesicles without Hb encapsulation at different temperatures, prepared as a counterpart model system of HbV. The raw small and wide angle scattering (SWAXS) data as obtained, shown in Figure 2a, confirm the absence of the so-called α-gel peak at q ~ 15 nm^{-1}, corresponding to interchain spacing of d = 0.42 nm, at all investigated temperatures. Although the α-gel-liquid crystalline phase transition temperature of DPPC is known to be 41 °C, this confirms a melted state of the hydrophobic chains in the lipid bilayers and high lateral fluidity of lipids even at 4 °C owing to the presence of cholesterol.

The (collimation corrected) absolute intensities after the background subtraction, $I(q)$, are displayed in Figure 2b as a function of temperature. As is well known, multilamellar stacks give equidistant peaks due to their structure factor. However, the low-q part (q < 0.3 nm^{-1}) of $I(q)$ exhibits neither an inter-bilayer interference peak nor its faint signature like an undulation. This finding indicates that as we designed, the structure of vesicle is, at least for the most part, uni-lamellar.

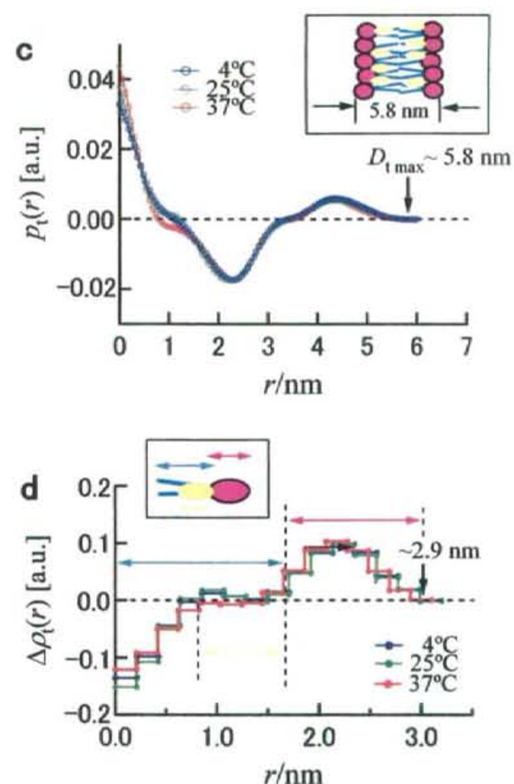

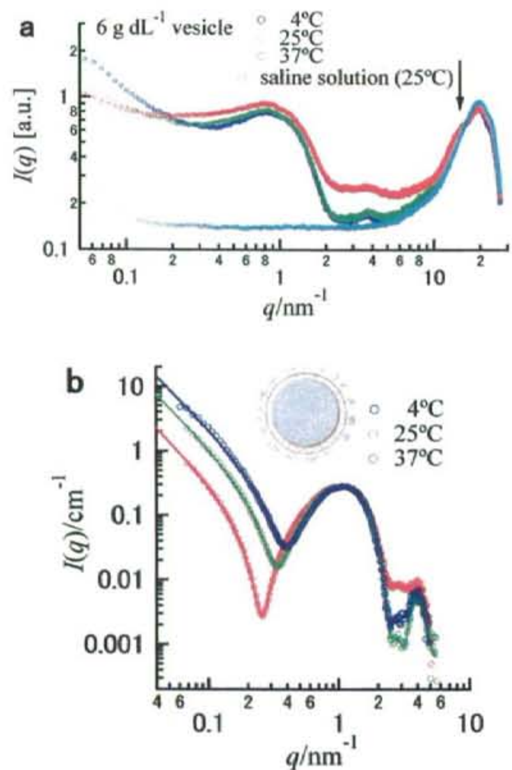

Figure 2: Structural characterization of a phospholipid bilayer membrane for Hb encapsulation as obtained by SAXS. Small and wide angle X-ray scattering (SWAXS) intensity in $0.05 \leq q/\text{nm}^{-1} \leq 27$ (a), collimation-corrected SAXS intensities on absolute scale (b), the thickness pair-distance distribution function, $p_t(r)$ (c), and electron density profile deconvoluted from $p_t(r)$ (d) of a 6 g dL^{-1} dispersion of the vesicle for Hb encapsulation as a function of temperature. In the insets of panel c and d, the structure of the lipid bilayer is schematically shown. A light blue line and a pink ellipse respectively represent hydrophobic chain and hydrophilic headgroup of the lipids, and a yellow ellipse stands for cholesterol.